

## Effect of wafer size on material removal rate and its distribution in chemical mechanical polishing of silicon dioxide film<sup>†</sup>

Hyunseop Lee<sup>1,\*</sup>, Yeongbong Park<sup>1</sup>, Sangjik Lee<sup>2</sup> and Haedo Jeong<sup>1</sup>

<sup>1</sup>*School of Mechanical Engineering, Pusan National University, San 30 Changjeon-dong, Kumjeong-ku, Busan 609-735, Korea*

<sup>2</sup>*Korea Institute of Industrial Technology, Jisa-dong, Gangseo-gu, Busan 618-230, Korea*

(Manuscript Received June 10, 2013; Revised July 3, 2013; Accepted July 29, 2013)

### Abstract

Chemical mechanical polishing (CMP) is a semiconductor fabrication process. In this process, wafer surfaces are smoothed and planarized using a hybrid removal mechanism, which consists of a chemical reaction and mechanical removal. In this study, the effects of wafer size on the material removal rate (MRR) and its uniformity in the CMP process were investigated using experiments and a mathematical model proposed in our previous research; this model was used to understand the MRR and its uniformity with respect to wafer size. Under constant process conditions, the MRR of a silicon dioxide (SiO<sub>2</sub>) film increased slightly along with an increase in wafer size. The increase in MRR may be attributed to the acceleration of the chemical reaction due to a rise in process temperature. Based on the results obtained, the  $k$  and  $\alpha$  values in the mathematical model are useful parameters for understanding the effect of wafer size on the MRR and its distribution under a uniform, relative velocity. These parameters can facilitate the prediction of CMP results and the effective design of a CMP machine.

*Keywords:* Chemical mechanical polishing (CMP); Material removal rate (MRR); MRR distribution; Mathematical modeling; Wafer size

### 1. Introduction

Chemical mechanical polishing (CMP) is a hybrid material removal process, which incorporates a chemical reaction and the mechanical removal of a dielectric film [1]. In the CMP process, material removal occurs by the synergetic cooperation of multiple process variables such as pressure, relative velocity, slurry flow, slurry chemical, and the material property of the abrasive. CMP technology plays an important role in realizing and miniaturizing high-performance integrated circuits (ICs) [2]. Nowadays, an improvement in productivity is achieved in the semiconductor industry through the use of large-sized wafers. However, in terms of global planarization, achieving uniform material removal has been a challenge in the CMP of large-scaled wafers.

The distribution of the material removal rate (MRR) in the oxide CMP process depends on the distribution of the normal contact stress of the wafer and the relative velocity between the wafer and the polishing pad [3]. Thus, previous studies have focused on calculating the stress distribution and relative velocity distribution.

Kim and Jeong [4] calculated the uniformity of the relative velocity distribution via kinematic analysis. They demonstrated that the ratio of the rotational velocity of the platen to that of the carrier governs the relative velocity distribution. Hocheng et al. [5] developed a material removal model for the CMP process, which is based on kinematic abrasive cutting. Normal contact stress distribution is also a key process variable for controlling the MRR distribution and has been studied by finite element analysis (FEA). Wang's [6] study on the stress distribution in the CMP process focused on the von Mises stress. However, Chen et al. [7] proposed that the normal contact stress in the CMP process due to friction force, which is related to the MRR, is proportional to the normal contact stress. Bae et al. [8] also demonstrated that the normal contact stress distribution is similar to the experimental MRR distribution in silicon dioxide (SiO<sub>2</sub>) CMP. Lee and Jeong [9], meanwhile, reported that the MRR distribution in copper CMP depends on the distributions of the normal contact stress, relative velocity, and chemical reaction. The effect of wafer size on the MRR distribution has yet to be investigated in sufficient detail although several studies have been conducted on the MRR distribution to explain the non-uniform material removal in CMP.

In this study, we used our previously proposed mathematical model [10] to compare the CMP performance for SiO<sub>2</sub>

\*Corresponding author. Tel.: +82 51 510 3210, Fax.: +82 51 518 8442

E-mail address: hyunseop.lee@gmail.com

<sup>†</sup>This paper was presented at the ICMDT 2013, Busan, Korea, May 2013.

Recommended by Guest Editor Haedo Jeong

© KSME & Springer 2013

wafers of different sizes. The model is also useful for gaining an understanding of factors affecting the MRR and its uniformity according to the scale-up of wafer size. We focused specifically on the effect of the normal contact stress distribution and wafer size on the MRR distribution.

## 2. Material removal rate distribution model

As mentioned above, we employed the semi-empirical MRR distribution model for the SiO<sub>2</sub> CMP, which has been proposed in our previous research [10], in order to understand the MRR and its uniformity with respect to wafer size. The normalized MRR distribution, considered as a spatial parameter ( $\phi$ ), can be expressed as a combination of the normalized stress distribution and the average relative velocity distribution [10], which is given by

$$\Omega(x, y) = \left\{ \left( \frac{\sigma_n(x, y)}{\sigma_{n,avg}} \right)^\alpha \left( \frac{V_{re,avg}(x, y)}{V_{re,avg}} \right)^\beta \right\} \quad (1)$$

where  $\sigma_n(x, y)$  is the normal contact stress at point  $(x, y)$  on the wafer;  $\sigma_{n,avg}$  is the average normal contact stress;  $V_{re,avg}(x, y)$  is the average relative velocity at position  $(x, y)$  on the wafer;  $V_{re,avg}$  is the average relative velocity of the wafer; and  $\alpha$  and  $\beta$  are indexes for representing the influence of each normalized parameter on the MRR distribution. The spatial parameter expresses the effect of each parameter on the formation of the MRR profile.

The average MRR of the wafer was modeled using the Greenwood-Williamson model [11] and contact mechanics [12]. In this study, we assumed that particle indentation into the polishing pad had elastic deformation and that the deformation associated with the wafer was fully plastic. The proposed semi-empirical MRR model for SiO<sub>2</sub> CMP based on Zhao and Chang's model [13] and Wang's nonlinear micro-contact model for a single particle [14] can be expressed as [10]

$$MRR_{avg} = \left[ \frac{4}{3} k \frac{\left( \sqrt{A_w^T} / l + 1 \right)^2}{A_w^T} \left( \frac{f_s}{C} \right) \left( \frac{R_p}{\sigma_p} \right)^{1/2} \right] \frac{PV_{re,avg}}{E_{pf}} \left( 1 - \frac{\xi}{2} \right)^{3/2} \int_{D_{cr}}^{+\infty} \Phi(D) D^2 dD \quad (2)$$

where  $A_w^T$  is the apparent wafer-pad sliding area, which is calculated from the total contact area between the rotating wafer and the polishing pad during the process time;  $k$  is a constant representing the effect of slurry chemicals;  $l$  is the distance between particles contained in the hypothetical slurry volume;  $f_s$  is the surface area density of the area of up-features of the grooved pad divided by the area of a flat pad;  $R_p$  is the average radius of curvature of the pad asperity tips;  $\sigma_p$  is the

standard deviation of the distribution of the pad asperity heights;  $P$  is the applied pressure;  $V_{re,avg}$  is the average relative velocity during the CMP process; and  $E_{pf} [E_{pf} = (1 - \nu_p^2)/E_p + (1 - \nu_f^2)/E_f^{-1}]$  is the composite elastic modulus of the pad ( $E_p$ ) and the film ( $E_f$ ), where  $\nu_p$  and  $\nu_f$  are the Poisson ratios of the pad and film, respectively. In addition,  $D$  is the diameter of the nanoparticle;  $D_{cr}$  is the critical particle diameter that can participate in the material removal process; and  $\Phi(D)$  is the size distribution of the particles in the CMP slurry. As reported in Jiang's study [15],  $C$  is approximately 0.35 in a typical CMP process. Here,  $l$  is calculated as [10]

$$l^3 - \left( \frac{2(A_w^T)^{3/2} + X}{A_w^T(N_p - 1)} \right) \cdot l^2 - \left( \frac{2(A_w^T)^{1/2}X + (A_w^T)^2}{A_w^T(N_p - 1)} \right) \cdot l - \left( \frac{X}{N_p - 1} \right) = 0 \quad (3)$$

where  $X$  is the total slurry volume,  $t_s$  is the imaginary slurry thickness ( $X/A_w^T$ ), and  $N_p$  is the total number of particles in the slurry.

Here,  $\xi$  is the ratio of the indentation depth of a particle into the polishing pad [ $\delta_p(D)$ ] to the particle diameter  $D$  [ $\xi = \delta_p(D)/D$ ]. According to Ref. [14],  $\xi$  can be obtained by

$$\left( \frac{H_f}{E_{ap}} \right)^2 = \frac{(4\xi + (2\xi - 1)(-3 + \sqrt{9 + 24\xi}))^2}{8\pi^2(2 - 2\xi)^2(-3 + \sqrt{9 + 24\xi})} \quad (4)$$

where  $H_f$  is the hardness of the film and  $E_{ap}$  is the composite elastic modulus of the pad and the particle.

Thus, the MRR distribution model can be written as

$$MRR(x, y) = MRR_{avg} \cdot \{\Omega(x, y)\} \quad (5)$$

## 3. Experimental

We conducted experiments wherein CMP was performed using a rotary CMP machine (GnP POLI762, GnP technology, Korea) designed for polishing 100 mm to 300 mm diameter wafers. An IC1000/SubaIV stacked polishing pad (Nitta Haas Inc., Japan), designed to improve the consistency of the CMP performance, was attached to the polishing platen. SiO<sub>2</sub> films were deposited on silicon wafers with diameters of 100, 150, 200, and 300 mm. The polishing time for each wafer was 60 s. The operating pressures were 27.58 and 34.47 kPa for the wafer and the retaining ring, respectively. The relative velocity was 65.312 m/min, and the slurry flow rate was 200 ml/min. The prepared slurry was a potassium hydroxide (KOH)-based silica slurry with a particle concentration of 12.5 wt%. The particle size distribution of slurry was measured using a particle-size analyzer.

During the CMP process, dynamic friction force and process temperature were measured using a CMP monitoring system equipped with a piezoelectric force sensor and an

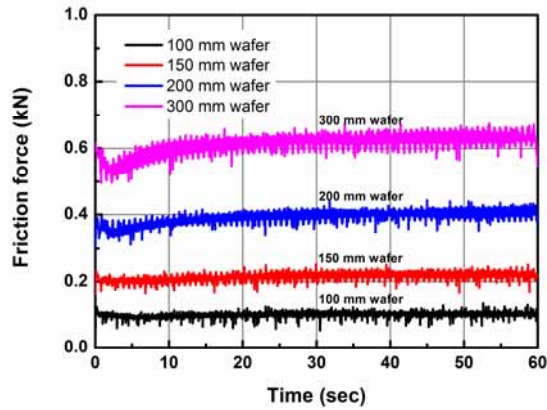


Fig. 1. Dynamic friction forces of wafers of various sizes during CMP process.

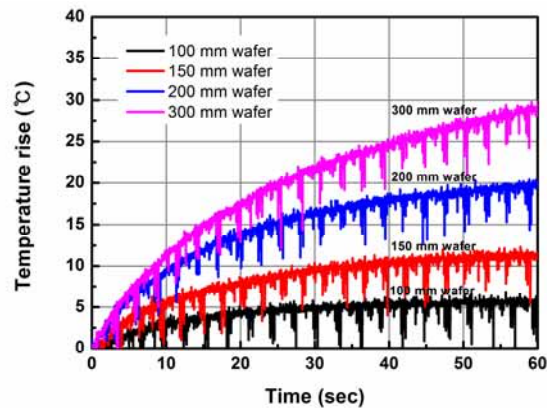


Fig. 2. Process temperature rise for wafers with various sizes during the CMP process.

infrared sensor. The initial temperature before CMP was controlled at  $20 \pm 1^\circ\text{C}$  for all experiments. The MRRs of wafers were measured using a reflectometer (K-Mac ST5030-SL). The initial thickness of the  $\text{SiO}_2$  film was 1500 nm for each wafer. The edge exclusion in the measurement of the MRR of the  $\text{SiO}_2$  film was 3 mm.

The normal contact stresses were obtained by FEA using commercially available ANSYS software (ANSYS Inc., Canonsburg, PA). The thicknesses of the wafers with diameters of 100, 150, 200, and 300 mm were 525, 675, 725 and 775  $\mu\text{m}$ , respectively. The 2D axisymmetric static model and material properties were as reported in Ref. [9].

#### 4. Experimental results and discussion

##### 4.1 Tribological characteristics

The friction force is known to be related to the MRR in the CMP process. Under a fixed wafer size, the MRR increases with increasing friction force [16]. However, a larger wafer size results in a higher friction force and higher polishing temperature under constant process conditions (Figs. 1 and 2).

The increases in friction and temperature are caused by the

Table 1. Average friction force and temperature rise of wafers of various sizes during CMP experiments.

Diameter (mm)	100	150	200	300
Avg. friction force (kN)	0.099	0.209	0.390	0.612
Avg. temperature rise ( $^\circ\text{C}$ )	4.7	9.3	15.1	25.5

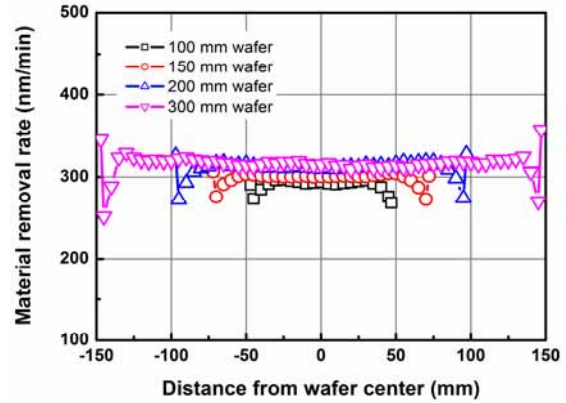


Fig. 3. MRR distribution of wafers with various sizes after CMP.

increase in normal force under the same pressure. The normal forces are 216.5, 487.1, 866.0, and 1948.5 N for the wafers with diameters of 100, 150, 200, and 300, respectively. The polishing temperature increases with the process time. The increase in polishing temperature affects the chemical reaction between the slurry chemicals and the  $\text{SiO}_2$  film. Despite the variation in the wafer diameters from 100 mm to 300 mm, the friction force and process temperature show a linear relationship (Table 1).

##### 4.2 Normal contact stress distribution

In this study, we used the same rotational velocities of the platen and wafer in order to ignore the effect of the relative velocity distribution on the MRR distribution. Under this condition of the same rotational velocities of the platen and wafer, the relative velocity is uniformly distributed on the wafer. This means that the second term on the right-hand side in Eq. (1) becomes “1.” Thus, in our experiments, the MRR distributions theoretically depended on the normal contact stress distribution with respect to wafer size.

Fig. 3 shows the MRR distributions of wafers of various sizes after the CMP process. The average MRRs of the wafers with diameters of 100, 150, 200, and 300 mm are 290.5, 298.6, 310.9 and 315.7 nm/min, respectively. The MRR of the  $\text{SiO}_2$  film increases slightly with increasing wafer size because of the impact of process temperature (Fig. 2). Under the application of pressure, the decrease and increase of the MRR near the wafer edge depend on the normal contact stress distribution resulting from the contact among the wafer, retaining ring, and polishing pad.

Meanwhile, Fig. 4 indicates that the deviation of normal contact stress decreases with an increase in wafer diameter,

Table 2. Material properties for mathematical modeling.

Variable	Value	Unit
$\sigma_p$	30	$\mu\text{m}$
$R_p$	25	$\mu\text{m}$
$E_p$	10	MPa
$\nu_p$	0.2	-
$E_a$	94	GPa
$\nu_a$	0.26	-
$\rho_a$	2270	$\text{Kg/m}^3$
$\rho_s$	1040	$\text{Kg/m}^3$
$E_f$	66	GPa
$\nu_f$	0.3	-
$H_f$	18	GPa

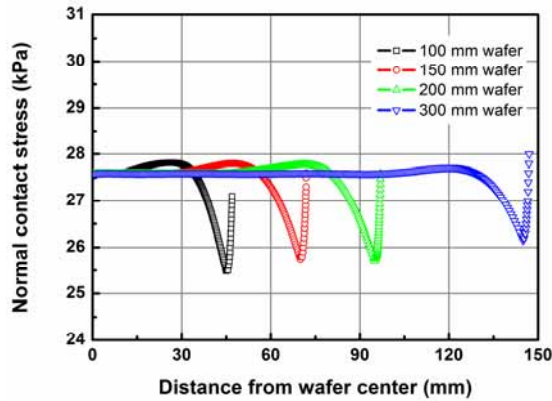


Fig. 4. Normal contact stress distribution of wafers with various sizes under pressure conditions of 27.58 kPa for the wafer and 34.47 kPa for the retaining ring (edge exclusion: 3 mm).

because the wafer thickness increases as the wafer diameter increases to avoid breakage from gravity sag while handling wafers. However, Fig. 3 shows that the deviation of MRR increases with an increase in the wafer diameter. The disagreement between the FEA results and the experimentally obtained MRR distribution can be attributed to the bow of wafers, which refers to the deviation of the center point of an unclamped wafer from the reference plane. Normally, the larger the wafer diameter, the larger the bow is (from  $\leq 10 \mu\text{m}$  for the wafer with a 100 mm diameter to  $\leq 40 \mu\text{m}$  for that with a diameter of 300 mm). The index  $\alpha$  in Eq. (1) compensates for the difference between the experimental MRR distribution and the normal contact stress; this index will be discussed later.

**4.3 Mathematical model and experimental results**

The material properties considered in our previous research [10] are listed in Table 2. From Eq. (5), it can be seen that the MRRs of the wafers with various sizes can be calculated considering the material properties listed in Table 2.

Here,  $D_{cr}$  is assumed to be 22 nm, and the  $k$  value is determined by comparing the results of the mathematical model with the experimental results [10]. The size distribution of slurry particles used in the CMP experiments is shown in Fig. 5. Assuming that  $k$  is “1” and the chemical reaction is ignora-

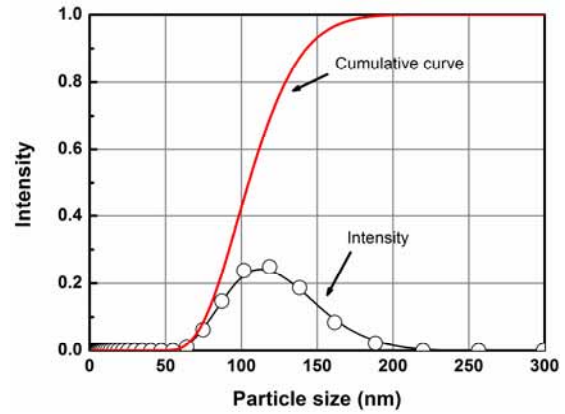


Fig. 5. Particle size distribution of slurry prepared for CMP experiment.

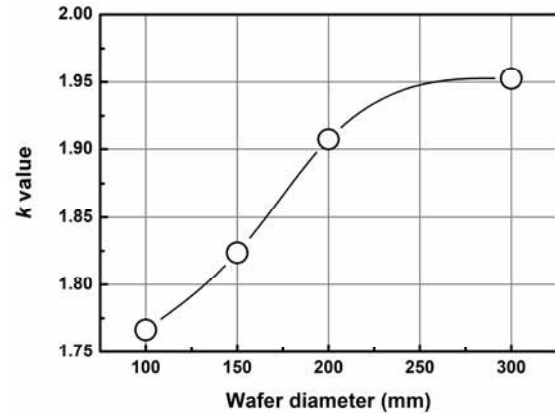


Fig. 6. The  $k$  values calculated from the comparison of mathematical model and experimental results as a function of wafer diameter.

ble, the MRRs resulting from only the mechanical removal by slurry particles (i.e., mechanical MRR by particles) can be calculated. The calculated MRR values are lower than the experimental values. As mentioned above, the experimental MRRs of the wafers with diameters of 100, 150, 200, and 300 mm are 290.5, 298.6, 310.9 and 315.7 nm/min, respectively. The experimentally obtained  $k$  values in Eq. (2), which indicate the chemical reaction effects calculated from the comparing the results of the calculated mechanical MRRs with the experimental results, increase with the increase in wafer size (Fig. 6). This implies that increasing the polishing temperature along with wafer size affects the chemical reaction between slurry chemicals and the  $\text{SiO}_2$  film.

Meanwhile, Fig. 7 shows the comparison of the normalized experimental and normalized theoretical MRR distributions. The  $\alpha$  values in Eq. (1) were derived from the linear regression of the normalized normal contact stresses and normalized MRRs. Assuming that the surfaces of the wafer and polishing pad are flat, as mentioned above, the deviation of the normal contact stress increases with a decrease in wafer diameter due to the difference in wafer thickness. The  $\alpha$  values for the wafers with diameters of 100, 150, 200, and 300 mm are 0.80, 1.42, 1.91 and 3.61, respectively. The theoretical MRR pro-

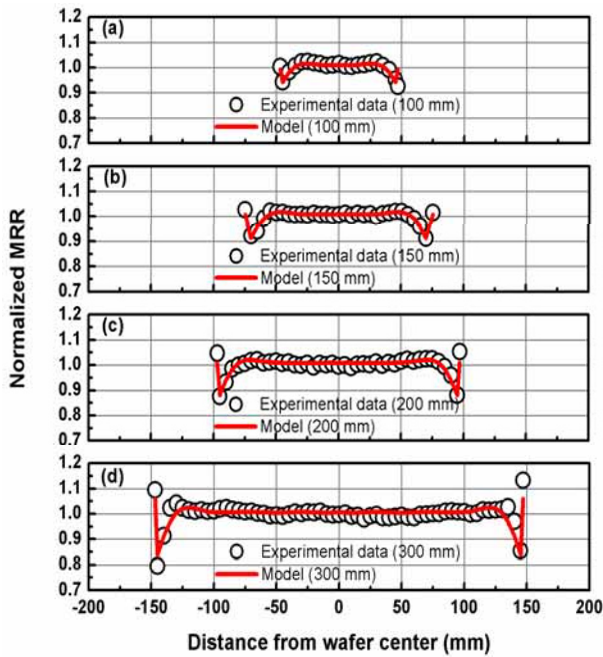


Fig. 7. Comparison of experimental and theoretical MRR distributions of wafers with various sizes: (a) 100; (b) 150; (c) 200; (d) 300 mm.

files are highly consistent with the experimental results (Fig. 7). The  $\alpha$  value compensates for the difference between the normalized normal contact stress distribution and experimental MRR distribution, by controlling the magnitude of the normalized normal contact stress. Moreover, the  $\alpha$  value increases with an increase in wafer size, thereby indicating that the bow size of the larger wafer is larger than that of a smaller wafer; consequently, the stress irregularity near the edge of a larger wafer is higher than that of a smaller wafer. Therefore, under a uniform, relative velocity distribution, the  $k$  and  $\alpha$  values in the mathematical model are the representative parameters for understanding the effect of wafer size on MRR and its distribution in our experiments. These parameters can be used for predicting the CMP results of the next generation 450-mm wafers.

### 5. Conclusions

In this study, we investigated the effect of wafer size on the MRR and its uniformity in the CMP process. Although the temperature difference is significant for the wafer size, we used experimental results and a previously proposed mathematical model to demonstrate that, under constant process conditions, the MRR of a SiO<sub>2</sub> film increases slightly with an increase in the wafer size because of the mechanical abrasion-dominant material removal mechanism of abrasives. The increase in MRR is a result of the acceleration of the chemical reaction due to the rise in process temperature. The  $k$  values in the mathematical model reflect the accelerated chemical reaction with the increase in wafer size. Under the condition of a uniform relative velocity, the  $\alpha$  value in the spatial parameter

compensates for the difference between the theoretical and experimental MRR distributions by controlling the magnitude of the normalized normal contact stress. Furthermore, the  $\alpha$  value increases with increasing wafer size, reflecting the geometrical characteristics of a wafer (e.g., the bow). Finally, the  $k$  and  $\alpha$  values in the mathematical model can be useful parameters for understanding the effect of wafer size on MRR and its distribution.

### Acknowledgment

The authors gratefully acknowledge the support of G&P Technology Inc. (Korea).

### Nomenclature

- $MRR_{avg}$  : Average material removal rate
- $\phi(x,y)$  : Spatial parameter
- $\sigma_n(x,y)$  : Normal contact stress at point  $(x,y)$
- $\sigma_{n,avg}$  : Average normal contact stress
- $V_{re,avg}(x,y)$  : Average relative velocity at position  $(x,y)$
- $V_{re,avg}$  : Average relative velocity of wafer
- $\alpha$  and  $\beta$  : Indexed for representing the influence of normalized parameters on MRR
- $A_w^T$  : Apparent wafer-pad sliding area
- $k$  : Constant representing chemical reaction
- $l$  : Distance among particles
- $f_s$  : Surface area density of polishing pad
- $R_p$  : Average radius of curvature of pad asperity
- $\sigma_p$  : Standard deviation of pad asperity heights
- $P$  : Applied pressure
- $E_{pf}$  : Composite elastic modulus of pad and film
- $D$  : Diameter of nanoparticle
- $D_{cr}$  : Critical particle diameter
- $\Phi$  : Particle size distribution
- $X$  : Total slurry volume
- $t_s$  : Imaginary slurry thickness  $(X/A_w^T)$
- $N_p$  : Total number of particle in the slurry
- $\zeta$  : Ratio of the indentation depth of particle into the polishing pad to the particle diameter
- $H_f$  : Hardness of film
- $E_{ap}$  : Composite Elastic modulus of pad and particle
- $MRR(x,y)$  : MRR distribution
- $E_p$  : Elastic modulus of pad material
- $\nu_p$  : Poisson's ratio of pad material
- $E_a$  : Elastic modulus of abrasive particle
- $\nu_a$  : Poisson's ratio of abrasive particle
- $\rho_a$  : Density of abrasive particle
- $\rho_s$  : Density of slurry
- $E_f$  : Elastic modulus of film material
- $\nu_f$  : Poisson's ratio of film material

### References

[1] H. S. Lee and H. D. Jeong, Chemical and mechanical bal-

- ance in polishing of electronic materials for defect-free surfaces, *CIRP Annals-Manufacturing Technology*, 58 (2009) 485-490.
- [2] H. Lee, S. Park and H. Jeong, Evaluation of environmental impacts during chemical mechanical polishing (CMP) for sustainable manufacturing, *J. of Mechanical Science and Technology*, 27 (2) (2013) 511-518.
- [3] D. Castillo-Mejia and S. Beaudoin, A locally relevant Prestonian model for wafer polishing, *J. of Electrochemical Society*, 150 (2) (2003) G96-G102.
- [4] H. Kim and H. Jeong, Effect of process conditions on uniformity of velocity and wear distance of pad and wafer during chemical mechanical planarization, *J. of Electronic Materials*, 33 (2004) 53-60.
- [5] H. Hocheng, H. Y. Tsai and M. S. Tsai, Effects of kinematic variables on nonuniformity in chemical mechanical planarization, *International J. of Machine Tools and Manufacture*, 40 (2004) 1651-1659.
- [6] D. Wang, J. Lee, K. Holland, T. Bibby, S. Beaudoin and T. Cale, Von Mises stress in chemical-mechanical polishing processes, *J. of Electrochemical Society*, 144 (1997) 1121-1127.
- [7] K. S. Chen, H. M. Yeh, J. L. Yan and Y. T. Chen, Finite-element analysis on wafer-level CMP contact stress: reinvestigated issues and the effects of selected process parameters, *International J. of Advanced Manufacturing Technology*, 42 (2008) 1118-1130.
- [8] J. Bae, H. Lee, S. Lee, Y. Guo, J. Park, M. Kinoshita and H. Jeong, Effect of Retainer Pressure on Removal Profile and Stress Distribution in Oxide CMP, *Proc. of International Conference on Planarization/CMP Technology*, Fukuoka, Japan (2009) 345-349.
- [9] H. Lee and H. Jeong, A wafer-scale material removal rate profile model for copper chemical mechanical planarization, *International J. of Machine Tools and Manufacture*, 51 (2011) 395-403.
- [10] H. S. Lee, H. D. Jeong and D. A. Dornfeld, Semi-empirical material removal rate distribution model for SiO<sub>2</sub> chemical mechanical polishing (CMP) processes, *Precision Engineering*, 37 (2013) 483-490.
- [11] J. A. Greenwood and J. B. P. Williamson, Contact of normally flat surfaces, *Proc. of the Royal Society A*, 95 (1966) 300-319.
- [12] K. L. Johnson, *Contact mechanics*, Cambridge, Cambridge University Press (1985).
- [13] Y. Zhao and L. Chang, A micro-contact and wear model for chemical-mechanical polishing of silicon wafers, *Wear*, 252 (2002) 220-226.
- [14] Y. Wang, Y. W. Zhao and J. Gu, A new nonlinear-micro-contact model for single particle in the chemical-mechanical polishing with soft pad, *J. of Material Processing Technology*, 183 (2007) 374-379.
- [15] J. Z. Jiang, Y. W. Zhao, Y. G. Wang and J. B. Luo, A chemical mechanical polishing model based on the viscous flow of the amorphous layer, *Wear*, 265 (2008) 992-998.
- [16] H. Lee, S. Joo and H. Jeong, Mechanical effect of colloidal silica in copper chemical mechanical planarization, *J. of Materials Processing Technology*, 209 (2009) 6134-6139.



sustainable manufacturing.



of semiconductors.



His research interests include ultra-precision machining and systems, process monitoring and simulation, and process integration and optimization.



received his Ph.D. degree in Mechanical Engineering from Tokyo University, Japan in 1994. His research fields include chemical mechanical polishing (CMP), grinding, polisher and consumable design, and post-CMP cleaning.

**Hyunseop Lee** received his B.S., M.S., and Ph.D. degrees in Mechanical Engineering from Pusan National University. He is currently a researcher at the School of Mechanical Engineering, Pusan National University, Korea. His studies include (chemical mechanical) polishing of electronic materials and

**Yeongbong Park** received his B.S. and M.S. degrees in Mechanical Engineering from Pusan National University, Busan, Korea in 2003 and 2009, respectively. He is currently a Ph.D. student in Mechanical Engineering from the same university. His research interest includes chemical mechanical polishing process

**Sangjik Lee** received his B.S. degree in Mechanical Engineering from Pusan National University, Busan, Korea, in 1997. He received his M.S. and Ph.D. degrees in Precision Mechanical Engineering from in the same university in 1999 and in 2010, respectively. He has been a Senior Researcher since 2010.

**Haedo Jeong** is a professor at the School of Mechanical Engineering at Pusan National University and a CEO of G&P Technology, Korea. He received his B.S. and M.S. degrees from Pusan National University and Korea Advanced Institute of Science and Technology (KAIST), respectively. Then, he